Studies on the Enzymatic Degradation of Solution-Grown Lamellar Crystals of Poly[(*R*)-3-hydroxybutyrate]: Defects in Crystals

Won-Ki Lee, Tadahisa Iwata, Hedeki Abe, and Yoshiharu Doi*

Polymer Chemistry Laboratory, RIKEN Institute, 2-1 Hirosawa, Wako-shi, Saitama 351-0198, Japan

Received June 12, 2000; Revised Manuscript Received October 20, 2000

ABSTRACT: Morphological changes during the enzymatic hydrolysis of solution-grown lathlike lamellar crystals (SGCs) of poly[(*R*)-3-hydroxybutyrate] (P(3HB)) attached on a silicon wafer have been studied in order to elucidate the initial stage of enzymatic attack by an extracellular PHB depolymerase purified from *Alcaligenes faecalis* T1. These changes may be interpreted in terms of the preferential erosion of less-ordered regions within the lamellae, parallel to the *b*-axis, resulting in breakup of lamellar crystals. The erosion continued along the *a*-axis from the edges of newly created crystal fragments. This initial hydrolytic behavior was confirmed by quenching samples from a series of temperatures (T_Q < melting temperature). At lower T_Q, ridges first appeared on the lamellar surface running parallel to the *b*-axis (width of crystal) and developed with increasing temperature. The ridge formation reflects the chain compression induced by the thermal molecular motion of less-ordered chains in lamellar crystals. The deformation of SGCs on poly(ethylene terephthalate) film by elongation has also been used to investigate the defect region in lamellar crystals. The multicracks of lamellae parallel to the *b*-axis were clearly observed after a *a*-axis elongation, while a *a*-axis compression accompanied by the elongation along the *b*-axis led to the ridge formation parallel to the *b*-axis on the lamellar surface, owing to pulling out of chains. All results suggest that the less-ordered chains within the lamellar crystals of P(3HB) exist along the *b*-axis mainly due to the lower regularity between chain-end groups.

Introduction

Degradable polymers are of growing interest in the areas of biomedical applications and polymer waste management caused by synthetic nondegradable polymers.[1−9] Polymer degradation occurs primarily in the hydrolyzable backbone linkages of the polymer chain, leading to a lower molecular weight and eventually to monomer regeneration. Well-known hydrolyzable polymers are polysaccharides,[1] polyesters,[2,6,10] poly(amino acids),[6] and polyanhydrides.[3,5] Among them, bacterially synthesized poly(hydroxyalkanoic acids) have attracted much attention as possible candidates for commercial biotechnological products.

The enzymatic degradation of poly[(*R*)-3-hydroxybutyrate] (P(3HB)) and its copolymers produced from renewable resources by bacterial fermentation has been extensively studied in solution-cast[11,12] and melt-crystallized films.[13,14] The results have revealed that the enzymatic degradation of P(3HB) preferentially occurred in the amorphous region and subsequently in the crystalline region. The chain-folded solution-grown lamellar crystals (SGCs) of P(3HB) have been used as a model system for elucidating the mechanism for both the enzymatic and hydrolytic degradation in the crystalline region in our laboratory[9,15−17] and by others.[18,19] P(3HB) crystallizes in a two-chain segment orthorhombic unit cell with parameters $a = 0.576$ nm, $b = 1.320$ nm, and c (fiber axis) $= 0.596$ nm.[20,21] SGCs of P(3HB) have been prepared from a number of solvent systems: chloroform/ethanol,[16,22] triacetin,[23] octanol,[23] propylene carbonate,[13,24] and poly(ethylene glycol).[25] The lamellar crystals were either single or multilayered lath-shaped lamellae, with the *a*-axis of the orthorhombic unit cell parallel to the long direction of the crystal, independent of the solvents used. In all cases, after partial degradation of SGC by extracellular PHB depolymerases, purified from *Alcaligenes faecalis* T1,[16] *Comamonas acidovorans* YM1609,[16] and *Pseudomonas lemoignei* Pha Z4,[19] the remaining crystals exhibited needle- or sawlike morphology along the long axis of the crystals; the chain scission predominantly takes place parallel to the average chain-folding direction at the extreme ends of lath-shaped crystals.[9,15−19] Thus, it is generally accepted that the behavior of enzymatic hydrolysis of SGCs is governed by the crystal structure and folding. Iwata et al.[16] and Nobes et al.[19] have suggested that the *endo*- and *exo*-type enzyme attack process may be a more effective mechanism for enzymatic hydrolysis when disordered regions exist within the lamellar crystal. Also, the needle- or sawlike crystal fragments of partially degraded SGCs have been explained by an edge attack model.

Since normal solution-grown crystals are not perfect, some regions in the lamellar crystals will be in a loose chain-packed state. Therefore, these regions will be more sensitive to enzymatic hydrolysis and thermal treatment. In this article, we attempt to obtain further insight into the enzymatic hydrolysis mechanism of SGCs. Hydrolysis experiments were conducted on nascent, thermally treated, and mechanically deformed crystals. The morphology of the crystals was studied by atomic force microscopy (AFM). The preferential erosion from central regions of P(3HB) lamellar crystals along the *b*-axis, not from the ends, at the initial stages of enzymatic hydrolysis is discussed in terms of the less-ordered chains (or defects) within the lamellar crystal.

Experimental Section

Preparation of Solution-Grown Crystals. The bacterial P(3HB) ($M_n = 380\,000$ and $M_w/M_n = 2.1$) was obtained from ICI (trade name: Biopol). The sample was purified by precipitation in excess *n*-hexane from a chloroform solution and dried in a vacuum. The low molecular weight P(3HB) ($M_n =$

* To whom correspondence should be addressed.

10.1021/ma001016c CCC: $19.00
Published on Web 12/01/2000

47 000 and $M_w/M_n = 1.6$) used in this study was prepared by a basic hydrolysis method, as reported previously.[15] Purified P(3HB) was dissolved in chloroform, and 1 N aqueous KOH and 18-crown-6 ether were added. The solution was stirred vigorously at 37 °C. The organic layer was extracted, dried over $MgSO_4$, and filtered. The resulting organic solution was precipitated in an excess of methanol and dried in a vacuum for 1 week. SGCs were prepared from an octanol-diluted solution, collected by centrifugation, washed with methanol several times, and then resuspended in methanol.

The samples were prepared by dropping crystal suspensions onto cleaned silicon wafers (3×3 mm^2) and poly(ethylene terephthalate) (PET) films (50×10 mm^2) for annealing and elongation experiments, respectively. After elongation of the PET films by stretching, the crystals attached to the PET film were deformed. The elongated film was glued onto a glass slide, and both edges were cut off.

Thermal Behavior and Thermal Treatment. The melting behavior of P(3HB) lamellar crystals was measured by DSC (Perkin-Elmer Pyris 1) under nitrogen and calibrated with indium as a standard material. The DSC thermograms were obtained at a heating rate of 20 °C/min, and the maximum of heat capacity peaks was taken as the melting temperature (T_m). Thermal treatments of SGCs on a silicon wafer were undertaken using DSC under nitrogen. A sample was heated to a desired temperature (T_Q) at a rate of 20 °C/min and then immediately quenched to −10 °C (with a cooling rate of at least 350 °C/min, which was enough to prevent recrystallization during cooling). The real temperature of samples on a silicon wafer was calibrated to within error of ±2 °C using a digital surface thermometer (Anritsu Meter Co.).

Enzymatic Hydrolysis. The enzymatic hydrolysis of both SGCs and their thermally treated samples was carried out on clean silicon wafers at 37 °C in 50 mM Tris-HCl buffer (pH 7.5). Samples were placed in a sterilized plastic cuvette containing 600 μL of buffer solution. The degradation was started by the injection of 0.5 μL (ca. 0.1 μg) of solution (209 μg/mL) of an extracellular PHB depolymerase purified from *Alcaligenes faecalis* T1. The reaction solution was incubated at 37 °C. In the case of the deformed crystals, the enzymatic hydrolysis was performed at room temperature. Samples were carefully washed with an excess of distilled water and dried in a vacuum.

AFM Studies. AFM measurements were conducted using a scanning force microscope and a SPA 300 instrument with SPI 3700 controller (Seiko Instrument Co.) at room temperature. The cantilever used in this study was triangular with a microfabricated Si_3N_4 microtip (Olympus Co.) and a spring constant of 0.022 N/m. The scanning direction was perpendicular to the long axis of the cantilever. Topographic and deflection images were carried out simultaneously in the repulsive force region (ca. 1 nN). Although the deflection image could not give information on the height, it is a useful mode to reveal the changes in the height of sample surface, especially when the sample surface is rough.

Results and Discussion

Enzymatic Hydrolysis by *Alcaligenes faecalis* T1 PHB Depolymerase. The solution-grown lamellar P(3HB) crystals (SGCs) were often aggregated, but individual lamellae were available for study at the periphery. Parts A and B of Figure 1 show respectively AFM topographic and deflection images of SGCs obtained from octanol solution, with multilamellar lath-shaped crystals grown from the aggregation center.

The enzymatic hydrolysis of SGCs of P(3HB) as a model substrate was first studied by Hocking et al.[18] using the PHB depolymerases from the fungus *Aspergillus fumigatus* and the bacterium *P. lemoignei*. Most studies on the enzymatic hydrolysis of SGCs have been carried out using the suspension method;[9,15−19] a PHB depolymerase is added to the buffer containing

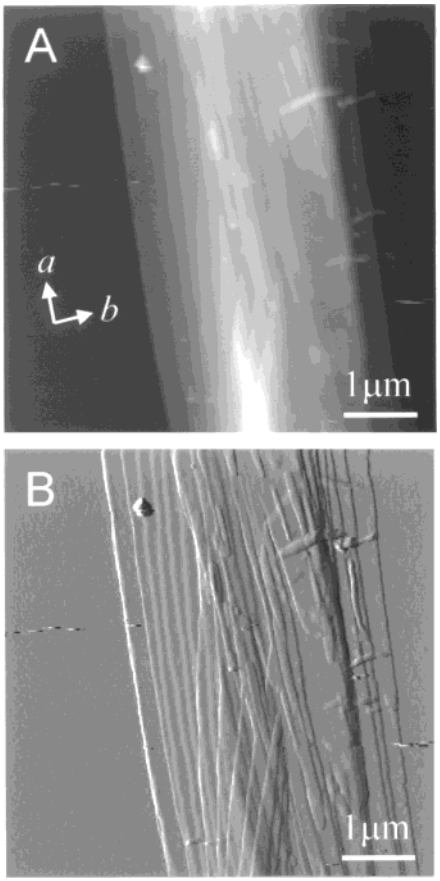

Figure 1. AFM topographic (A) and deflection (B) images of solution-grown P(3HB) crystals.

SGCs, and after incubation, the remained crystals are collected by centrifugation, similar to the method of crystal collection described in the Experimental Section. Although this method has provided valuable data on enzymatic hydrolysis of SGC, the measured morphological data mainly provide information on the main body of the crystals. Accordingly, if some crystal fragments are separated from the original crystals due to the hydrolysis, it is difficult to observe lamellar morphological changes during hydrolysis. The experimental method applied to this study provides better opportunities to observe the morphological changes caused by hydrolysis, because the crystals are attached to a silicon wafer as a substrate, before, during, and after hydrolysis.

From extensive TEM studies performed on the enzymatic hydrolysis of SGCs, it is known that the hydrolysis by an enzymatic attack progresses from the edges and along their long axes rather than the chain-folding surfaces; this mechanism yields crystal fragments with narrow cracks or splinters.[16,19] The observation of narrow cracks in the enzymatically degraded SGCs was explained in terms of the chain-folding structure and its direction. To obtain more insight into the mechanism of enzymatic hydrolysis of SGC, short and long hydrolysis times were applied to SGC on a silicon wafer. Parts A and B of Figure 2 show the deflection images of SGCs after 4 and 60 min of enzymatic hydrolysis, respectively, at 37 °C by an extracellular PHB depolymerase purified from *A. faecalis* T1. The image after 4 min of hydrolysis (Figure 2A) shows the initial stage of erosion within the lamellae which takes place predominantly in the central region along the *b*-axis, even though most reports on the enzymatic hydrolysis of SGCs suggested that the

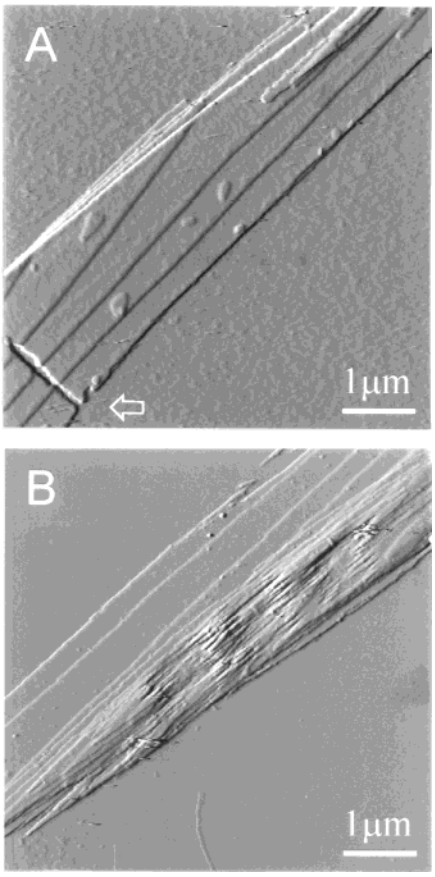

Figure 2. Deflection images of solution-grown lamellar crystals after 4 min (A) and 60 min (B) of enzymatic hydrolysis at 37 °C by an extracellular PHB depolymerase purified from *A. faecalis* T1. The arrow indicates an initial erosion along the *b*-axis.

degradation preferentially occurs at the crystal ends along the *a*-axis.[16,19]

As the hydrolysis time is increased, however, the image in Figure 2B shows small crystal fragments with narrow cracks along the *a*-axis at the topmost lamellae, as reported previously.[16,19] A noticeable feature of this image is that the original edges and the lamellae, located at bottom (on silicon substrate), remain close to their original shapes. These morphological results suggest that the initial stage of enzymatic hydrolysis leads to a breakup of the lamellar crystal along the crystallographic *b*-axis and produces small crystal fragments. As the enzymatic hydrolysis proceeds along the *b*-axis, perpendicular attack along the average chain-folding direction (*a*-axis) also starts on the freshly created edges. Further hydrolysis creates small crystal fragments with narrow cracks as usually reported (see Figure 2B).[16,19] These morphological observations support the hypothesis that the enzymatic hydrolysis of SGCs occurs by a combination of slower *endo*- and faster *exo*-chain scissions. The mechanism of the enzymatic hydrolysis of SGC suggested by these morphological results is schematically represented in Figure 3.

Thermal Properties of SGCs. The thermal properties of SGCs were investigated using DSC. A SGC mat (ca. 1 mg) was prepared by filtering the solution suspension using a vacuum pump in order to minimize the effect of thermal history. This SGC mat was heated in the DSC from −20 to 190 °C at 20 °C/min (Figure 4A). After kept for 1 min at 190 °C, the sample was cooled to −20 °C at a cooling rate of 350 °C/min and

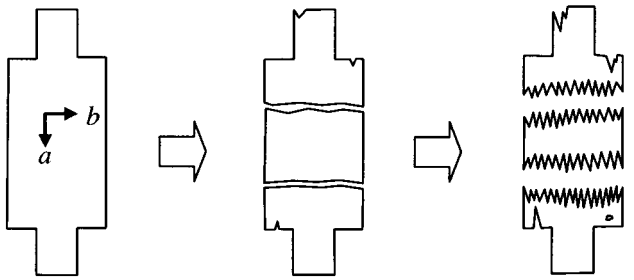

Figure 3. Schematic representation of the enzymatic hydrolysis of solution-grown lamellar crystals by an extracellular PHB depolymerase purified from *A. faecalis* T1.

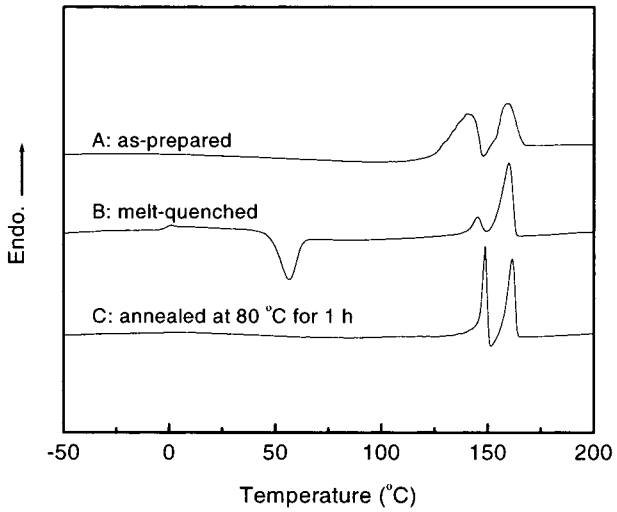

Figure 4. DSC thermograms of solution-grown P(3HB) crystals with/without thermal treatment.

then reheated at 20 °C/min (Figure 4B). Figure 4C shows the DSC trace of the annealed mat after 1 h at 80 °C. All three thermograms exhibited double melting peaks. This is common for P(3HB) and is a consequence of recrystallization; the lower peak (T_L) corresponds to the melting of original crystals, while the higher peak (T_H) is due to the remelting of new crystals during heating.[26,27] The exotherm from the recrystallization was shown in the thermogram of Figure 4C where the minimum between both the peaks dropped below the baseline. Thus, it is difficult to determine the T_m of original crystals because the endothermic peak partially overlaps the exothermic one from the recrystallization. Once the crystals have been melted, the thermal behavior is similar to that obtained from the original polymer.

The endotherm of T_L in the first heating run corresponds to the melting of the SGCs and was unexpectedly broad, from 115 to 147 °C. This broad melting behavior may be due mainly to the packing rearrangement of crystals. Other important factors could be considered as a difference in crystal sizes and imperfections within the crystals. Because the AFM morphological studies reported here are focused on the well-organized SGCs, the effects of voids and crystal sizes should not have significant impact on the observed enzymatic hydrolysis.

It has been reported that the crystallinity of SGCs is about 80%, or possibly even higher.[7] Since the crystallinity of SGCs used in this study is about 78% (as estimated by wide-angle X-ray diffraction), this lower crystallinity is thought to emanate partly from small crystal sizes and imperfections within crystals. The enzymatic hydrolysis initially occurs at the defects in

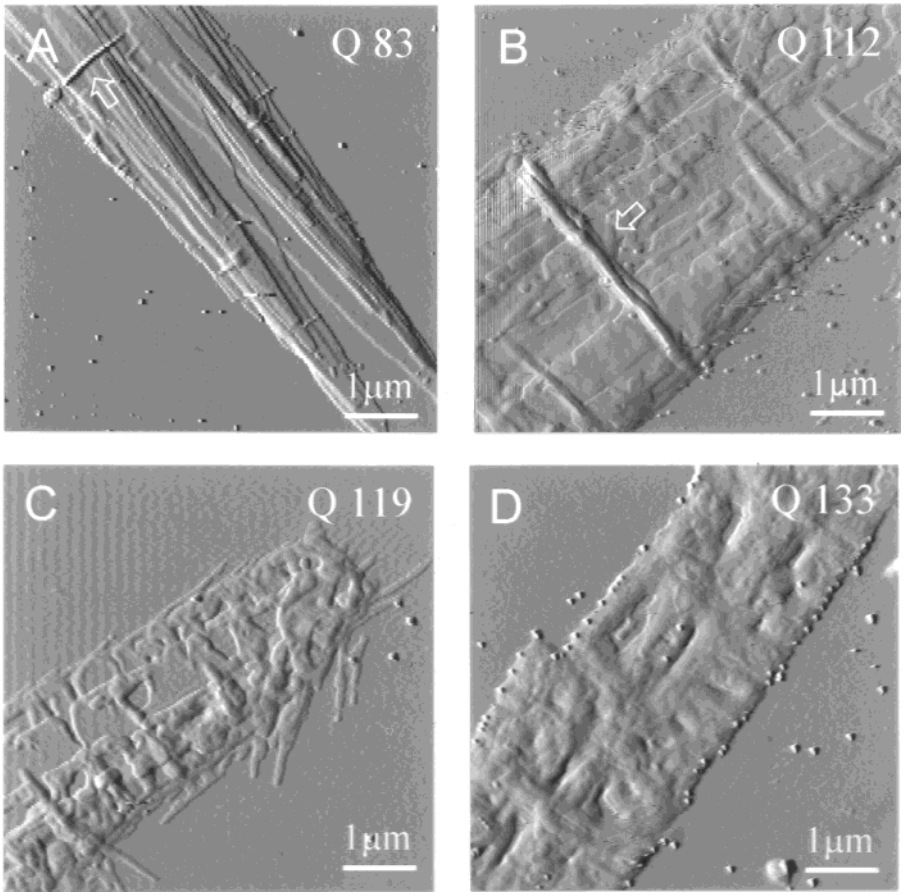

Figure 5. Deflection images of solution-grown P(3HB) crystals after quenching at various temperatures (T_Q) (A, 83 °C; B, 112 °C; C, 119 °C; D, 133 °C). The arrows indicate the ridges.

the lamellar crystals. Because of the difference in thermal molecular mobility (or viscoelastic property) between ordered and less-ordered regions within the lamellar crystals, we expect that the regions of less-ordered and well-ordered chains in the lamellar crystals may be distinguished by the thermal treatment at temperatures lower than T_m.

Thermal Behavior of SGC and Enzymatic Hydrolysis. The glass transition temperature (T_g, P(3HB): 4 °C) is manifested by the motion of molecular backbone segments usually in amorphous regions. Thus, at temperatures above T_g, but below T_m, the molecular motion of segments in crystal lattices is related to their conformational stability. Therefore, if the initial erosion due to the enzymatic attacks reflects the chain regularity within the lamellar crystals, the lamellar crystals may contain less-ordered and more thermally sensitive regions.

To investigate thermally induced morphological changes in the lamellar crystals, a series of thermal treatment experiments of SGCs at T_Q between T_g and T_m were performed using DSC. The deflection images of the SGCs of P(3HB) quenched at different T_Qs are shown in Figure 5. After the quenching from 83 °C, small ridges perpendicular to the long axis (*a*-axis) of the lamellar crystal were observed, as indicated by the arrow. The ridges became more distinct at a T_Q of 112 °C, and their width and length increased. This is interpreted in terms of the crystal compression due to the active molecular motion of loosely packed regions in the lamellar crystals. Heterogeneous melting was also observed, mainly at the edges of lamellar crystals. In addition, a holelike morphology was observed on the surface at T_Qs of 112 and 119 °C due to the melting of the less-ordered chains located inside the lamellar crystals. Further heating to 133 °C resulted in the melting of lamellar surface (see Figure 5D), even though the T_m of SGCs is around 139 °C. The thermally induced morphological trends are similar to the initial hydrolytic behavior shown in Figure 2A. Thus, it seems reasonable that the thermally induced morphological results of the SGCs reflect the packing state of chains in the lamellar crystals.

Since preferential hydrolysis occurs in the less-ordered regions within lamellae, the thermally induced ridges is expected to show faster hydrolysis due to the chain irregularity. Figure 6 shows the deflection images of the thermally treated SGCs after 10 min of enzymatic hydrolysis at 37 °C. As expected, the ridges were preferentially degraded, and the erosion regions became broader on increasing TQ. All images also included a holelike morphology on the lamellar surface, related to the surface erosion mentioned previously. Therefore, we have concluded that the enzymatic hydrolysis of these SGCs at the initial stage occurs not only at edges but also at less-ordered chain packing regions on crystal surface.

Plastic deformation in the remaining ridges induced by the AFM tip scanning, as shown in Figure 6B, gives additional evidence regarding the change in the mechanical property of thermally induced ridges. When the tip slides over a polymeric surface, the sample surface can be easily deformed when it is rubbery or when the applied force is high. Since the whole surface was scanned under the same experimental conditions, tip-induced deformation was observed only on the ridges.

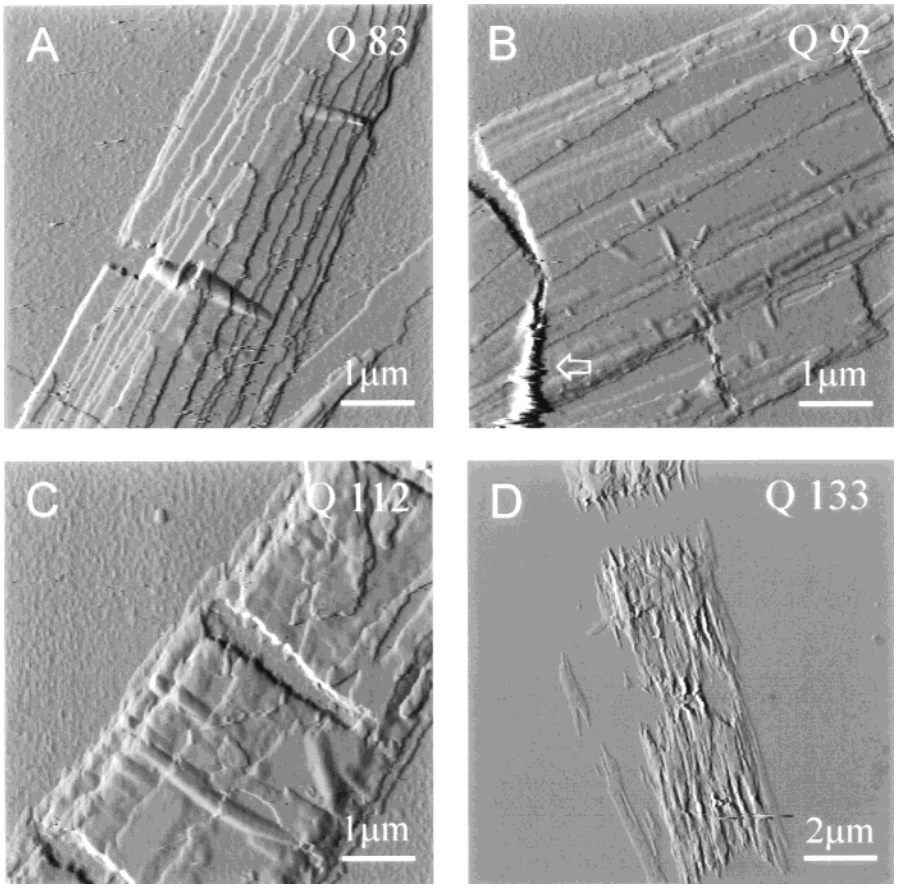

Figure 6. Deflection images of thermally quenched solution-grown crystals after 10 min of enzymatic hydrolysis at 37 °C by an extracellular PHB depolymerase purified from *A. faecalis* T1. The arrow indicates a plastic deformation induced by the AFM tip.

Thus, the ridges must be more amorphous or more rubberlike than the rest of the surface.

Figure 6D shows crystal fragments with narrow cracks, similar to the morphology of SGCs hydrolyzed for 60 min (see Figure 2B). This indicates that the core crystal structure remained intact, even though the thermally treated lamellar surface was essentially melted.

Deformation of SGCs and Enzymatic Hydrolysis. To further understand the chain-folding direction and crystallographic stability under stress, the crystals were placed on PET thin film and stretched at room temperature. By elongating the PET film, microcracks may develop along a specific crystallographic plane or in a loosely packed region of the crystals. A microfibrillar texture across the cracks can be observed, if the degree of polymerization is sufficiently high to maintain continuity of chains across the cracks, i.e., chain bridges.

Figure 7A shows the AFM topographic images of the crystals after an elongation of 10% along the *a*-axis of crystal. Multiple cracks were found almost perpendicular to the elongation direction. A similar morphology has been observed in the lamellar crystals of P(3HB)[13] and syndiotactic polypropylene,[28] when the crystals are placed on a Mylar film and stretched both perpendicular and parallel to the crystallographic *a*-axis. In this experiment, linear ridges parallel to the elongation direction were observed as shown in Figure 7B. This result can be explained by the compression of the PET film. When a film is elongated along one direction, its width along the perpendicular direction is decreased. No obvious microcracks perpendicular to the elongation direction could be found. This is consistent with the result reported by Barham et al.,[13] who observed that periodic cracks intersecting the elongation direction developed in lamellae elongated up to 50%. The mean width of cracks after the *a*-axis elongation was similar to the elongation ratio, whereas the *b*-axis elongation was noticeably lower. This result indicates that the interchain force caused by the packing states along the *b*-axis is higher than along the *a*-axis due to the weakness between the chain-end groups. Therefore, this weak packing along the *a*-axis may cause the cracking parallel to the *b*-axis.

The AFM topographic images in Figure 8 show the SGCs after deformation along the *a*- or *b*-axis, followed by 10 min of enzymatic hydrolysis at room temperature. After enzymatic degradation at room temperature, the cracks running parallel to the *b*-axis of crystal induced by the *a*-axis elongation can be observed to broaden (in comparison with Figures 7A and 8A). This observation reflects the fact that the chains at newly created crack edges have less-ordered structures, some of which originally existed in the lamellae and some of which were produced by stress, resulting in faster hydrolysis by the enzyme.

Although we could not observe cracks running along the *a*-axis before enzymatic degradation (Figure 7B), a narrow crack running along the *a*-axis and cracks almost along the *b*-axis could be observed as shown in Figure 8B. The width of cracks running along the *b*-axis is broader than that along the *a*-axis. This result is very similar to the ratio of elongation to deformation for the *a* and *b* directions observed by Barham et al.,[13] again suggesting that the cohesive energy between adjacent chains along the *a*-axis is stronger than that along

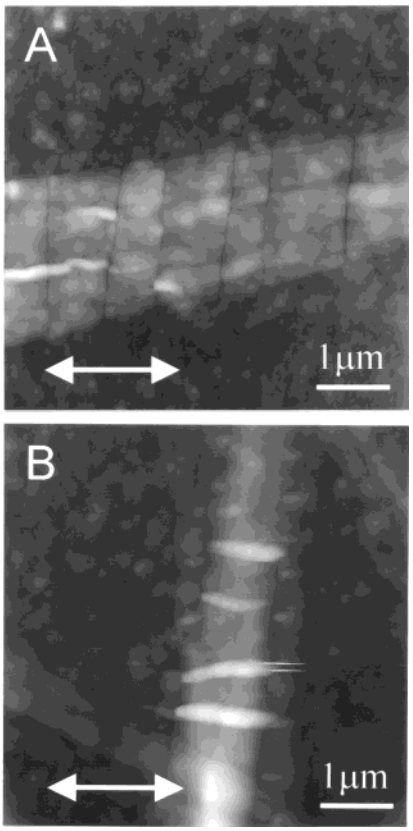

Figure 7. AFM topographic images of solution-grown P(3HB) crystals after 10% elongation parallel (A) and perpendicular (B) to the *a*-axis of crystal. The double arrows indicate the elongation direction.

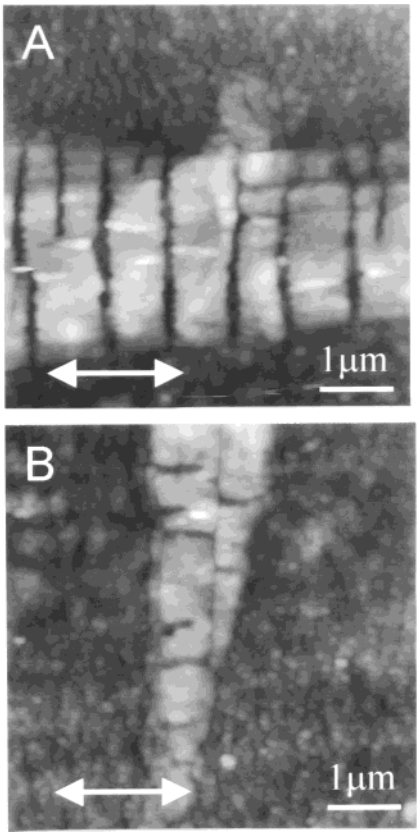

Figure 8. AFM topographic images of deformed solution-grown P(3HB) crystals after 10% elongation parallel (A) and perpendicular (B) to the *a*-axis of crystal, followed by 10 min of enzymatic hydrolysis at room temperature by an extracellular PHB depolymerase purified from *A. faecalis* T1. The double arrows indicate the elongation direction.

b-axis. If a defect in the original crystal is present, it makes the regular folding of adjacent chains difficult (neighboring effect). This might offer linear hydrolysis at the initial stage and ridge formation parallel to the *b*-axis. Furthermore, the chains were cropped out from the crystal along the *b*-axis, when the crystal was compressed during the elongation or crystal was applied to thermal treatment. These suggest that a less ordered region exists along the *b*-axis, which is more sensitive to both thermal and enzymatic attack.

Conclusions

The enzymatic hydrolysis of solution-grown chain-folded lathlike crystals (SGCs) of P(3HB) has been investigated using atomic force microscopy in order to elucidate the mechanism of enzymatic attack by an extracellular PHB depolymerase purified from *A. faecalis* T1. The measurements were performed on crystals attached to a silicon wafer and have allowed us to visualize the initial stage of the enzymatic hydrolysis. The results of both enzymatic hydrolysis and thermal treatment of SGCs are consistent. A short hydrolysis time (4 min) leads to the breakup of lamellae parallel to their short axis (crystallographic *b*-axis). Similarly, ridge formation appears along the *b*-axis at low quenching temperature. Additional evidence to support the initial behavior of enzymatic hydrolysis was found from the morphological changes caused by deformation of crystals. The ridge formation could be observed along the *b*-axis in the lamellar crystals. This suggests that a less ordered region exists along the *b*-axis, which is more sensitive to both thermal and enzymatic attack. The proposed model offers a better understanding for studying the initial stages of enzymatic hydrolysis of P(3HB) crystals.

Acknowledgment. The authors thank Prof. E. Atkins for helpful discussion. This research was supported in part by the grant for Ecomolecular Science Research, RIKEN Institute, provided by the Science and Technology Agency (STA) of Japan and a Grant-in-Aid for Scientific Research on Priority Area, "Sustainable Biodegradable Plastics", No. 11217216 (1999), from the Ministry of Education, Science, Sports and Culture, Japan.

References and Notes

(1) Chanzy, H.; Comtat, J.; Dube, M.; Marchessault, R. H. *Biopolymers* **1979**, *18*, 2459.
(2) Fredericks, R. J.; Melveger, A. J.; Dolegiewtz, L. J. *J. Polym. Sci., Polym. Phys. Ed.* **1984**, *22*, 57.
(3) Ron, E.; Mathiowitz, E.; Mathiowitz, A.; Domb, A.; Langer, R. *Macromolecules* **1991**, *24*, 2278.
(4) Nijenhuis, A. J.; Grijpma, D. W.; Pennings, A. J. *Macromolecules* **1992**, *25*, 6419.
(5) Hayashi, T. *Prog. Polym. Sci.* **1994**, *19*, 663.
(6) Scott, G.; Gilead, D. *Degradable Polymers*; Chapman & Hill: London, 1995.
(7) Birley, C.; Briddon, J.; Sykes, K. E.; Barker, P. A.; Organ, S. J.; Barham, P. J. *J. Mater. Sci.* **1995**, *30*, 633.
(8) Tsuji, H.; Ikada, Y. *Polymer* **1995**, *36*, 2709.
(9) Iwata, T.; Doi, Y. *Macromolecules* **1998**, *31*, 2461.
(10) Chu, C. C. *J. Appl. Polym. Sci.* **1981**, *26*, 1727.
(11) Doi, Y.; Kitamura, S.; Abe, H. *Macromolecules* **1995**, *28*, 4822.
(12) Abe, H.; Doi, Y. *Macromolecules* **1996**, *29*, 8683.
(13) Barham, P. J.; Keller, A.; Otun, E. L.; Holmes, P. A. *J. Mater. Sci.* **1984**, *19*, 2781.

(14) Abe, H.; Doi, Y.; Aoki, H.; Akehara, T. *Macromolecules* **1998**, *31*, 1791.
(15) Iwata, T.; Doi, Y.; Kasuya, K.; Inoue, Y. *Macromolecules* **1997**, *30*, 833.
(16) Iwata, T.; Doi, Y.; Tanaka, T.; Akehata, T.; Shiromo, M.; Teramachi, S. *Macromolecules* **1997**, *30*, 5290.
(17) Iwata, T.; Doi, Y.; Kokubu, F.; Teramachi, S. *Macromolecules* **1999**, *32*, 8325.
(18) Hocking, P. J.; Marchessault, R. H.; Timmins, M. R.; Lenz, R. Z.; Fuller, R. C. *Macromolecules* **1996**, *29*, 2472.
(19) Nobes, G. A. R.; Marchessault, R. H.; Chanzy, H.; Briese, B. H.; Jendrossek, D. *Macromolecules* **1996**, *29*, 8330.
(20) Okamura, K.; Marchessault, R. H. In *Conformation of Biopolymers*; Ramachandran, G. N., Ed.; Academic Press: New York, 1967; Vol. 2, p 709.
(21) Yokouchi, M.; Chatani, Y.; Tadokoro, H.; Teranishi, K.; Tani, H. *Polymer* **1973**, *14*, 267.
(22) Lundgren, D. G.; Alper, R.; Schnaitman, C.; Marchessault, R. H. *J. Bacteriol.* **1965**, *89*, 245.
(23) Lauzier, C.; Marchessault, R. H.; Smith, P.; Chanzy, H. *Polymer* **1992**, *33*, 823.
(24) Welland, E. L.; Stejny, J.; Hatler, A.; Keller, A. *Polym. Commun.* **1989**, *30*, 302.
(25) Revol, J.-F.; Chanzy, H. D.; Deslandes, Y.; Marchessault, R. H. *Polymer* **1989**, *30*, 1973.
(26) Owen, A. J.; Heinzel, J.; Skrbic, Z.; Divjakovic, V. *Polymer* **1992**, *33*, 1563.
(27) de Koning, G. J. M.; Scheeren, A. H. C.; Lemstra, P. J.; Peeters, M.; Reynaers, H. *Polymer* **1994**, *35*, 4598.
(28) Bu, Z.; Yoon, Y.; Ho, R.; Zhou, W.; Jangchud, I.; Eby, R. K.; Cheng, S. Z. D. *Macromolecules* **1996**, *29*, 6975.

MA001016C